"Maximal Credible Accident" Simulation Studies at the Storage Ring of the APS

G. Decker, A. L. Justus, P. K. Job, H. J. Moe, J. H. Vacca and V. R. Veluri

September 1997

Introduction:

The Advanced Photon Source (APS) is designed to be a major national user facility providing high-brilliance x-ray beams. Figure 1 shows a plan view of the APS. The main feature of the APS facility is the Experiment Hall building, which houses a 7-GeV storage ring within a concrete-shielding enclosure. The ring is capable of supporting 35 bending magnet and 35 insertion device beamlines for synchrotron radiation research. Either positrons or electrons can be stored in the storage ring and maintained in a circular orbit. The supply of particles is provided by the APS injector system consisting of the linac system, a positron accumulator ring (PAR), a 7-GeV synchrotron, and associated beam transfer lines. The standard mode of operation will use positrons.

The storage ring tunnel is constructed of ordinary concrete and high density concrete. It provides shielding for the radiation which is produced when positrons are lost around the ring. The outer wall of the tunnel is in the form of a ratchet which allows the photon beamlines to exit the tunnel into the Experiment Hall through the radial part of the ratchet wall (see Figure 2). The photon beam leaving the tunnel enters an area called the first optics enclosure (FOE). The FOE houses the equipment used in the synchrotron radiation experiment.

The tunnel houses the technical components which constitute the lattice for storing the positron beam in an orbit of 1104 m circumference. The beam height is 1.4 m above the floor, and the height of the tunnel is 2.74 m with a varying width of 2.74-4.5 m, due to the ratchet sections. The roof shield over the tunnel is 1 m of ordinary concrete (ρ = 2.35 g/cc), and the inner wall of the tunnel is 0.8 m of ordinary concrete. The ratchet walls are 0.56 m of high density concrete (ρ = 3.8 g/cc), up to a height of 2.13 m, and above that height, ordinary concrete. The bulk shielding design was based on the methodology available in published literature (SWA 79, SWA 85, FAS 84), using experimental data for attenuation lengths and expressions for the angular distribution of radiation (DIN 77, JEN 79). The details of the bulk shielding calculations for all the components of the APS have been documented (MOE 91, MOE 94).

Objective:

This study was aimed at determining the adequacy of the storage ring bulk shielding for reducing the radiation hazard outside of secured areas, due to errant particle beam losses. The DOE Order 5480.25 (DOE 92) requires that an accelerator facility determine and document the adequacy of the shielding for errant particle beams. Additionally, the hazard class (Low, Medium or High) of an accelerator is determined by the onsite and offsite effective dose equivalent under the assumption of a "maximal credible accident" occurring. The credible

maximal accident condition is that which produces at the weakest part of the shielding at full power the greatest amount of radiation at the subject position outside the secured area during one hour. For the hazard class to be Low, the onsite radiation level must be between 1 and 25 rem (10-250 mSv) in the one hour duration of the maximal credible accident. The safety envelope defines the bounding conditions for the safe operation of a DOE accelerator facility. The APS safety envelope for injection is stated as a limit on the power in watts. The safety envelope for the storage ring in injection mode is 308 W. This is equivalent to operating the injector synchrotron with 20 nC per pulse at a 2-Hz repetition rate, and at an energy of 7.7 GeV. For the stored beam case, the safety envelope is stated as a limit of 9280 J of stored energy. By obtaining measurements of dose rates at low power levels during the missteering operations, these can be extrapolated to the expected dose rates at the safety envelope power level. This allows one to compare the calculated dose consequences of the maximal credible incident with those obtained by extrapolation of the actual measurements.

Measurement Methodology:

For normal operating conditions, one would expect losses in the storage ring to occur primarily in the injection septum and at the transition section at the beginning of an insertion device (ID). However, in the event the beam becomes missteered, the loss could occur anywhere in the ring. It is conservatively assumed for the maximal credible accident in the storage ring that the beam is lost during injection in the high dispersion region (see Figure 2; AS4) in one of the forty sectors. This region is about 4 m long and includes four quadrupoles with a sextupole at the center. Calculations were made by semi-empirical methods (MOE 94) and indicated the highest dose, 10.7 rem (107 mSv), for this missteering incident for the assumed one hour duration would occur in the FOE directly outside the shielding tunnel. Additional calculations were made for beam losses at AQ2 and BQ2, but the results turned out to be less than that for AS4. Controlled beam loss studies were conducted using the injected beam at reduced intensity, at less than 3.5% of the power delivered at the safety envelope (DEC 95). The beam was transported into the straight section of each sector; the appropriate vertical corrector magnets were energized and the beam missteered. This scenario was repeated for as many sectors as possible. The missteered beam propagated for approximately 20 m downstream of a vertical corrector before striking the vacuum chamber wall. Radiation measurements were made in the Experiment Hall, paying special attention to ratchet doors, on top of the storage ring (mezzanine), and in the utility corridor on the infield side. Measurements were made at all straight penetrations into the tunnel. These locations were scanned, and the highest measured reading was recorded.

The Health Physics instruments used in this study consisted of instruments with known response to pulsed fields down to 1 pps. The Eberline RO-20, a portable 220-cc air ionization chamber, was used to measure photon fields. It responds acceptably up to at least 200 mR/h (2 mSv/h) per pps. In addition, photon fields were measured using the Victoreen 450P, a portable 240-cc pressurized (8 atmospheres) N_2 + Ar ionization chamber, which also responds acceptably up to at least 200 mR/h (2 mSv/h) per pps. Tests performed at the ANL Chemistry linac indicated a usable response up to 2.7 R/h (27 mSv/h) per pps for both of

these instruments. Neutron fields were measured using the Health Physics Instruments HPI-2080 pulsed-neutron remmeter. This neutron remmeter consists of a 10-inch-diameter polyethylene pseudosphere with two centrally located GM tubes. One tube is silver wrapped and the other is tin wrapped. The response to a gamma field will be approximately the same in each tube. The neutron activation of the silver wrapping is used to measure the neutron contribution to the dose. Gamma compensation is obtained by subtracting the activity in the tin-wrapped tube from the total activity in the silver-wrapped tube. In pulsed neutron/gamma fields, the gamma compensation is very effective at fields ≥ about 0.7 mR/h (7 μSv/h) per pps. Pulsed neutrons of any pulse repetition rate are measured acceptably up to 300 mrem/h (3 mSv/h) with this instrument (BRO 80).

Results:

The missteering studies were conducted around the entire storage ring. The measured results were extrapolated to dose rates at the safety envelope of 308 W. Table 1 shows only selected results of the controlled missteering beam loss studies. The entries in Table 1 represent the highest dose rates measured in the vicinity of the indicated locations. Figure 2 shows a

Table 1. Selected Results from the Storage Ring Controlled Beam Loss Studies
(Extrapolated to Dose Rate at the Safety Envelope)

Beam Loss Location	Dose Point Locations			
	Utility Corridor (rem/h)*	Mezzanine (rem/h)	Experiment Hall (rem/h)	Comments
S1AV1	1.465	0.014	0.35	(2ID Door)
S2BV1	0.088	0.033	0.23	(2ID Door)
S4AV1	1.055	0.025	0.18	(3ID Door)
S4BV1	0.047	0.012	0.23	(3ID Door)
S5AV1	1.465	0.023	0.23	(4ID Door)
S5BV1	0.041	0.014	0.35	(5ID Door)
S10AV2	1.468	0.073	1.47	(10BM Wall)
S13AV2	9.542	0.073	0.73	(13BM Door)
S23AV2	1.884	0.031	0.88	(23BM Wall)
S24AV2	1.10	0.035	1.72	(24BM Door)
S32BV4	6.38	0.286	2.20	(32BM Wall)
S34AV2	6.688	0.132	2.29	(33BM Wall)
S35BV4	3.08	0.088	0.88	(35BM Wall)
S40VV1	0.66	1.10	0.016	
S40VV3	0.825	0.165	0.084	

* multiply table value by 10 for mSv/h

typical portion of a sector where the beam was lost. The locations, in the Experiment Hall, of dose points used in the calculations are indicated for the incidents for AQ2, AS4, and BQ2. The doses mentioned above are under the assumption that the missteered beam continues in its course for one hour unattended. In reality, the machine is expected to shut down in no more than a few seconds if such missteering actually occurs.

In Table 1, the results for all sector locations ending in AV1 or AV2 represent losses on the fifth girder of a sector (corresponding to BQ2 in Figure 2). The highest dose rates measured in the Experiment Hall ranged from 0.18 - 2.29 rem/h. The semi-empirical calculation for the BQ2 incident gave a result of 7.24 rem/h, which is conservative by a factor of about 3 - 40, not accounting for the missed high-energy neutron dose component. Part of the variation in the measured results can be attributed to the presence of additional shielding by the front end components at some of the loss locations. Results for the sector locations ending in BV1 are for losses on the third girder (corresponding to AS4 in Figure 2). The highest measured dose rates varied from 0.23 - 0.35 rem/h, compared to the calculated result of 10.7 rem/h. This is conservative by a factor of 30 - 45. Sector locations ending in BV4 represent losses on the first girder (corresponding to AQ2 in Figure 2). The highest measured dose rates varied from 0.88 - 2.2 rem/h, compared to the calculated value of 6.0 rem/h, conservative by a factor of 2.7 - 6.8. The large measured values in the utility corridor were mostly obtained at straight penetrations through the wall, which are about 2.5 m above the floor level. Moreover, entry to this region is restricted while the machine is running and is not allowed at all during injection.

Another controlled loss study done was the loss of the beam on a transition region between the storage ring vacuum chamber and the ID vacuum chamber (see Figure 3). The transition piece is a copper interface between the two vacuum chambers, tapered from a 4-cm opening down to 1.2 cm. Photon/neutron doses outside the shielding wall were estimated using a combination of the EGS4, PICA, and 1-dimensional ANISN codes (JOB 95) and the semi-empirical methods (MOE 94). The measurements were made for the continuous-injection loss of a low power beam. Two experiments were performed. The first used a corrector magnet, adjacent to the transition piece, at full strength to deflect the beam into the transition piece. The second directed the beam onto a closed gate valve just upstream of the transition piece. In both cases, data were collected for 5 - 10 minutes while the charge entering the storage ring through the beam line transfer section was integrated electronically. The measured and calculated results are shown in Table 2.

Table 2. Experimental and Calculated Dose Rates for Losses on a Transition Piece during Continuous Injection (Extrapolated to the Safety Envelope Power)

	Neutron Dose Rate rem/h*	Gamma Dose Rate rem/h
Experiment #1	1.06	0.06
Experiment #2	1.58	0.044
PICA	2.20	0.04
Semi-Empirical	1.15	7.02

* multiply table value by 10 for mSv/h

The experimental results seem to suggest that more showering takes place in experiment #2 than in experiment #1. If this is the case, then a significant portion of the gamma radiation continues on in the forward direction. This would explain why the gamma dose in each of the experiments and the PICA calculation are so much lower than that of the semi-empirical calculation. Additionally, the PICA calculation only assumed one-third of the shower was contained in the transition piece. However, in the semi-empirical calculation all of the shower was assumed to occur in the transition piece. The uncertainty in the amount of showering which takes place at the loss site greatly affects the gamma dose rates, since most of the gamma radiation proceeds in the forward direction at very small angles. The energy distribution of the neutrons which penetrate the shield is poorly known. Hence, the relative agreement in the experimental and calculated results may be somewhat suspect, since it is not known what fraction of the medium and high energy neutron components that are slowed down are detected by the neutron instrument. Moreover, the neutron instrument does not respond to neutrons above 20 MeV. So, it is also unknown how much of the medium- and high-energy dose contribution is actually being missed.

Conclusions:

The measured dose rate results at each location showed wide variations, which tends to indicate that the missteered beam may not have hit at the same point for each repeat of a given loss scenario. However, all measured results were comfortably below the calculated values. It appears the use of semi-empirical calculational methods are generally quite conservative, which is desirable for perceived beam loss accidents at the safety envelope.

With respect to the disagreement between the calculated dose rates and the measured values for the "maximal credible accident," we suspect that the actual showering which takes place is more distributed along the beamline than the 4-m-long beam spill assumed in the calculations. Since the distribution is not known, this adds further to the difficulty in correlating the measured results with the calculated values.

In all controlled loss studies, it appears that the measured results were obtained for showers that may not have been fully developed. This means that a large fraction of the radiation is lost in the tunnel downstream from the loss point and does not contribute to the dose at dose point(s) outside of the bulk shielding or to the regions where most of the measurements were obtained.

References:

BRO 80 Brown, D., Buchanan, R.J., Koelle, A.R. "A Micro-Computer Based Portable Radiation Survey Instrument for Measuring Pulsed Neutron Dose Rates," Health Phys., **38**:507(1980).

DEC 95 Decker, G., internal documents, January 1995.

DOE 92 Department of Energy, Safety of Accelerator Facilities, DOE Order 5480.25, Washington, D.C. (Nov. 3, 1992).

DIN 77 Dinter, H. and Tesch, K. "Dose and Shielding Parameters of Electron-Photon Stray Radiation from a High Energy Electron Beam," Nucl. Inst. Meths. **143**:349 (1977).

FAS 84 Fasso, A., Goebel, K., Hofert, M., Rau, G., Schonbacher, H., Stevenson, G. R., Sullivan, A. H., Swanson, W.P., Tuyn, J. W. N. "Radiation Problems in the Design of the Large Electron-Positron Collider (LEP)," CERN 84-02 (1984).

JEN 79 Jenkins, T. M., "Neutron and Photon Measurements Through Concrete from a 15-GeV Electron Beam on a Target - Comparison with Models and Calculations," Nucl. Inst. Meths. **159**:265 (1979).

JOB 95 Job, P. K. and Gabriel, T. A., "Photoneutron Yield Predictions by PICA and Comparison with Experiments," Proc. of the Specialists Meeting on Shielding Aspects of Accelerators, Targets and Irradiation Facilities, CERN, Geneva, Switzerland, Oct. 12-13, 1995, pp. 93-96 (1995).

MOE 91 Moe, H. J., "Advanced Photon Source Radiological Design Considerations," APS-LS-141 Revised, Argonne National Laboratory, Argonne, IL (1991).

MOE 94 Moe, H. J., internal document to G. Decker, July 31, 1994.

SWA 79 Swanson, W.P., Radiological Safety Aspects of the Operation of Electron Linear Accelerators, Technical Report Series No. 188, IAEA, Vienna (1979).

SWA 85 Swanson, W. P., De Luca, P. M., Otte, R.A., Schilthelm, S.W., "Aladdin Upgrade Design Study: Shielding," University of Wisconsin (1985).

FIGURE 1. LAYOUT OF THE APS

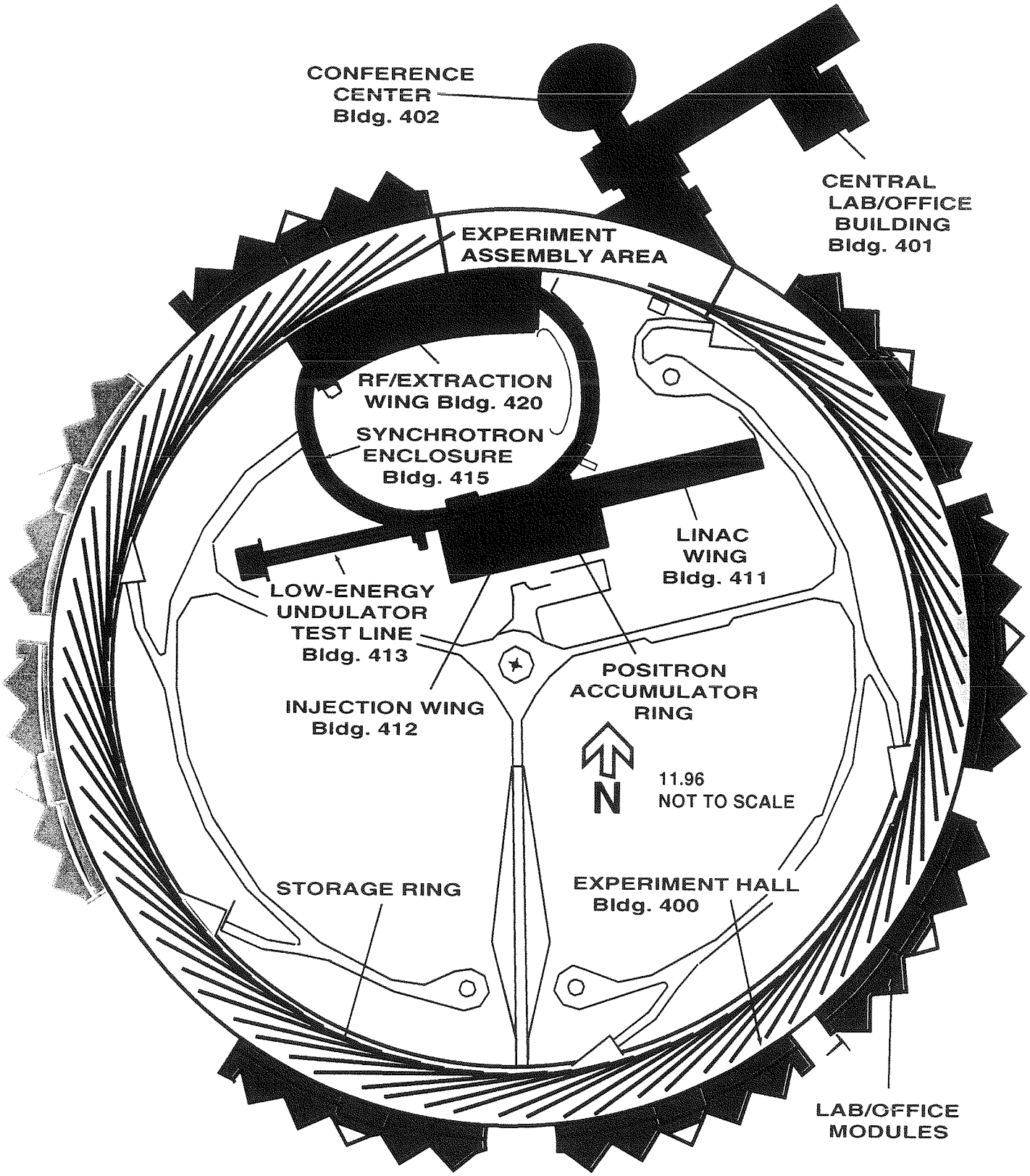

FIGURE 2. BEAM LOSS AREAS & DOSE POINT LOCATIONS

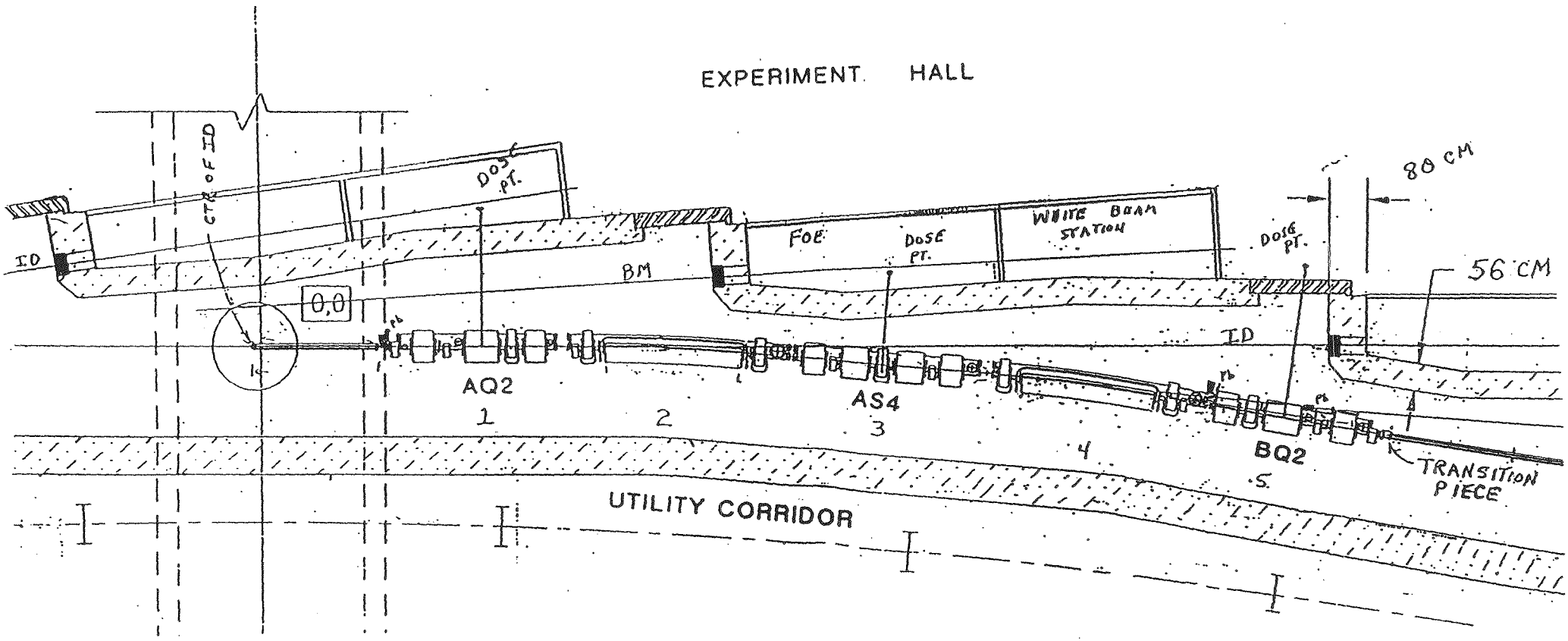

FIGURE 3. TRANSITION REGION BEAM LOSS POINT
& DOSE POINT LOCATIONS